



Strål
säkerhets
myndigheten

Swedish Radiation Safety Authority

Author: Magnus Dahlberg
Dave Hannes
Zhouwang Chen

Research

2016:28

Fatigue fracture surface
characterization and investigation

SSM perspective

Background

In a previous study (SSM research report 2015:38) fatigue experiments were performed on welded austenitic stainless steel piping components. The fatigue experiments offer an opportunity to examine the obtained fatigue cracks with an optical microscope.

Objective

The present study performs a fractographical examination of the obtained fatigue cracks with the aim of determine where fatigue cracks initiate and how the fatigue cracks propagate in the welded austenitic stainless steel pipes.

Results

The study has increased the understanding of fatigue critical points in welds, as well as it has increased knowledge on where fatigue cracks initiated and how propagation occur in the welded austenitic stainless steel pipes. The main results from the study are:

- Fatigue cracks were initiated from both the inside and outside of the weld joint.
- Fatigue initiation from the outside of the weld joint (weld toe) occurred predominantly at low cycle fatigue.
- Fatigue initiation from the inside of the weld joint (weld root) occurred predominantly at high cycle fatigue.
- High cycle fatigue life was not affected by the presence or the quality of the weld cap since the fatigue cracks started from the weld root.

Project information

Contact person SSM: Fredrik Forsberg

Reference: SSM2015-3856



Strål
säkerhets
myndigheten

Swedish Radiation Safety Authority

Author: Magnus Dahlberg, Dave Hannes, Zhouwang Chen
Inspecta Technology AB, Stockholm, Sweden

2016:28

Fatigue fracture surface characterization and investigation

Date: September 2016

Report number: 2016:28 ISSN: 2000-0456

Available at www.stralsakerhetsmyndigheten.se

This report concerns a study which has been conducted for the Swedish Radiation Safety Authority, SSM. The conclusions and viewpoints presented in the report are those of the author/authors and do not necessarily coincide with those of the SSM.

Title: Fatigue fracture surface characterization and investigation
Author: Dave Hannes, Magnus Dahlberg, Zhouwang Chen
Inspecta Technology AB,
Stockholm Sweden
Date: 2016-08-24

Summary

Fatigue experiments have previously been performed on a realistic welded austenitic stainless steel piping components in a study aiming at investigating the margins of the ASME design fatigue curve for austenitic stainless steel. The test specimens had therefore been subjected to constant and variable amplitude loads at both low and high cycle fatigue. The results were reported in Evaluation of fatigue in austenitic stainless steel pipe components – SSM 2015:38. In the present study the previous investigation was complemented with a fractographical examination of the obtained fatigue cracks for each of the 28 thin-walled welded piping components using an optical microscope.

The study improved understanding of fatigue critical points in welds, as well as it increased knowledge on where fatigue cracks initiated and how propagation occurred in welded austenitic stainless steel pipes. The regions more likely to suffer from fatigue initiation in the considered piping component were identified as being the weld toes on both the inside and outside of the weld joint. Two distinct fatigue failure mechanisms with separate initiation sites and distinct fatigue crack shapes were identified: fatigue initiation from the outside of the weld joint occurred predominantly at low cycle fatigue, whereas fatigue initiation from the weld root was the dominant fatigue failure mechanism at high cycle fatigue.

The examination also contributed to improved understanding of the link between weld quality and fatigue resistance. The weld joint was fatigue tested in as-welded condition. Weld cap removal is expected to be beneficial to increase low cycle fatigue life. The presence of a weld face toe did indeed localize fatigue initiation from the outside. The presence or quality of the weld cap did however not affect high cycle fatigue life, where fatigue cracks started from the weld root. In this case, it is the weld root quality that affected the fatigue life. The significance for both initiation and propagation of fatigue cracks of weld residual stresses introduced by a welding operation was highlighted. The observations are highly relevant for the selection of effective weld joint quality improvements aiming at increasing fatigue resistance of the welded piping component.

Sammanfattning

Utmattningsprov har utförts på svetsade austenitiska rostfria rör för att undersöka marginalerna i ASME:s design utmattningskurva för austenitiskt rostfritt stål. Provtavarna utsattes för cyklisk belastning med konstant och variabel amplitud, både vid låg- och högcykelutmattning. Resultaten redovisades i *Evaluation of fatigue in austenitic stainless steel pipe components* - SSM 2015: 38. I den aktuella studien kompletteras den förra undersökningen med en fraktografisk analys av utmattningssprickorna som uppstod under provningen av de 28 tunnväggiga svetsade rören.

Studien ökade förståelse för kritiska punkter för utmattning i svetsar och bidrog till ökad kunskap om var utmattningssprickor initieras och hur de växer i svetsat austenitiskt rostfritt stål. Både in- och utsidan av svetsen visade sig vara områden för initiering av utmattningsskador. Två olika initieringsställen och distinkta sprickformer identifierades: sprickinitiering från utsidan av svetsen inträffade främst vid lågcykelutmattning, medan sprickinitiering från svetsroten var den dominerande skademekanismen vid högcykelutmattning.

Studien har också bidragit till ökad förståelse av sambandet mellan svetskvalitet och utmattningshållfasthet. Svetsen utmattningsprovades utan slipning. Borttagning av svetsrågen förväntas vara fördelaktigt för att öka livslängden vid lågcykelutmattning. Förekomsten av en svetstå bidrar nämligen till att lokalisera utmattningsinitiering från utsidan. Förekomsten eller kvaliteten på svetsrågen påverkade dock inte livslängden vid högcykelutmattning, där utmattningssprickorna initierade från svetsroten. I detta fall är det svetsrotens kvalitet som påverkar utmattning livslängden. Betydelsen av svetsegensspänningar, som uppstår vid en svetsoperation, för både initiering och propagering av utmattningssprickor diskuterades. Iakttagelserna i den aktuella studien är av stor betydelse för valet av kvalitetsförbättringar i syfte att öka utmattningshållfasthet av svetsade rör.

Contents 2016:28

| | | |
|----------|--|-----------|
| 1 | NOMENCLATURE | 4 |
| 2 | INTRODUCTION | 5 |
| 2.1 | BACKGROUND | 5 |
| 2.2 | PERFORMED PIPING COMPONENT FATIGUE TESTS | 5 |
| 2.3 | OBJECTIVES | 8 |
| 3 | FRACTOGRAPHIC STUDY | 9 |
| 4 | RESULTS | 10 |
| 4.1 | FATIGUE INITIATION | 10 |
| 4.2 | FATIGUE PROPAGATION | 17 |
| 4.2.1 | <i>Fatigue Crack Shape at Leakage.....</i> | <i>17</i> |
| 4.2.2 | <i>Fatigue Crack Interaction</i> | <i>18</i> |
| 5 | DISCUSSION..... | 19 |
| 6 | CONCLUSIONS | 20 |
| 7 | RECOMMENDATIONS | 21 |
| 8 | ACKNOWLEDGEMENT | 21 |
| 9 | REFERENCES | 22 |

1 Nomenclature

| | |
|-------------------|--|
| l | Crack length, circumferential dimension of fatigue crack |
| N | Total number of cycles, experimental fatigue life |
| r, φ, z | Cylindrical coordinate system introduced in Figure 2 |
| R_i | Internal radius of specimen |
| t | Wall thickness of specimen |
| β | Exponent in Basquin equation |
| ε | Strain |
| ε_a | Strain amplitude |
| ■ _{in} | Value on the inside of the specimen |
| ■ _{init} | Value corresponding to initiation |
| ■ _{max} | Maximum value |
| ■ _{out} | Value on the outside of the specimen |

2 Introduction

2.1 Background

The ASME Boiler and Pressure Vessel Code, Section III [1] specifies rules for construction of nuclear facility components and includes mandatory design fatigue curves for different materials. Such design curves are typically obtained through adjustment of a mean curve derived from experimental data. The data used in the determination of such a mean curve generally results from experiments performed in laboratories on small, smooth specimens in air. The correction of the mean curve resulting in the design curve intends to overcome the fundamental problem of transferability to real components. Component testing or fatigue experiments under more realistic conditions including different environmental, material or loading effects allow to validate the margins in the ASME design fatigue curves and in particular quantify the degree of conservatism.

The margins of the design fatigue curve for austenitic steel in [1] were investigated with an experimental study, using 28 welded austenitic stainless steel pipe components [2]. This study contributed with:

- increased understanding of the ASME margins by highlighting extensive conservatism in the ASME fatigue procedure.
- improved knowledge on fatigue in austenitic stainless steel components and the fundamental issue of transferability.
- the development of an experimental procedure for fatigue testing of a realistic component allowing for more realistic margins and component specific design curves.
- highlighting the importance of using realistic variable amplitude (VA) loading to obtain reliable design curves, as opposed to using constant amplitude (CA) testing.

The different achievements of the performed work aimed at improving control of potential fatigue risks in piping components.

2.2 Performed Piping Component Fatigue Tests

The 28 test specimens in [2] had been manufactured from seamless TP 304 LE stainless steel pipes joined with a circumferential single v-joint butt weld, see Figure 1 (a). At the vicinity of the circumferential butt weld the nominal wall thickness (t) and inner diameter ($2R_i$) measured respectively 3 mm and 49.25 mm. The welding joints were in as-welded condition. All of the 28 test specimens have been verified and approved with a radiographic examination.

All piping components were fatigue tested at room temperature and subjected to reversed bending loading with displacement control in a standard single axis servo-hydraulic testing machine. The nominal axial strain was recorded with a strain gage situated in the bending plane. The experimental set-up was based on the inventive construction using custom-built fixtures, see Figure 1 (b). The piping components were during fatigue testing pressurized with water at 70 bar. Fatigue failure was defined by leakage, i.e. when the internal pressure could no longer be sustained.

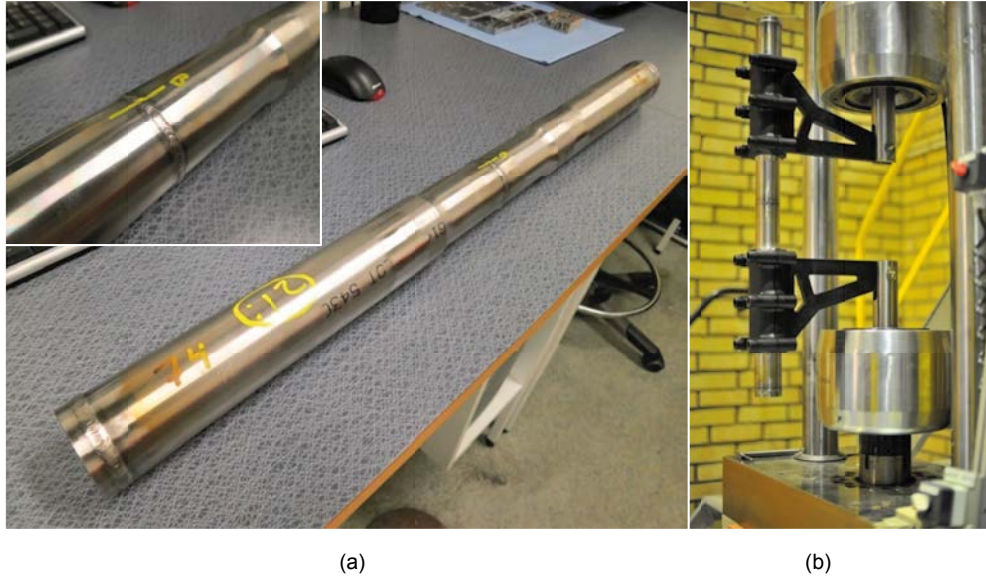


Figure 1 (a) Welded piping component with close-up view of the circumferential butt weld in as welded condition. (b) Actual mounted test specimen in servo-hydraulic testing machine.

The study had particular focus on high cycle fatigue (HCF) and variable amplitude loading. The fatigue experiments included both constant amplitude fatigue tests and experiments with variable amplitude loading using one out of three different load spectra:

- a piping spectrum (VAP), based on characteristic piping loads,
- a Gaussian spectrum (GAP), based on the piping spectrum, and
- a two-level block spectrum (VA2).

Each type of loading was performed at different severities for the considered loading types, except for the VA2 loading where only one severity was considered, see also Table 1.

Table 1 Summary of different load types considered in the fatigue experiments performed in [2].

| Load type | | Total number of performed tests | Number of tested severities |
|-------------------------|-----|---------------------------------|-----------------------------|
| Constant amplitude (CA) | | 10 | 6 |
| Variable amplitude | VAP | 7 | 4 |
| | VAG | 6 | 3 |
| | VA2 | 5 | 1 |

Additional information about the test specimens, experimental set-up, testing procedure and/or load description are presented in [2, 3]. Some selected fatigue results obtained for the 28 considered specimens are summarized in Table 2, where the total number of load cycles N , the maximum nominal strain amplitude $\max \varepsilon_a$ and the beta-norm $\|\varepsilon_a\|_\beta$ computed with $\beta = 4.6$, are reported. Both strain measures are based on the recorded nominal strain and the definition of the beta-norm is detailed in [2].

Table 2 Selected fatigue results from the performed fatigue tests in [2].

| Pipe ID | Load type | Severity ^(*) | N [cycles] | $\max \varepsilon_a$ [%] | $\ \varepsilon_a\ _\beta$ [%] |
|---------|-----------|-------------------------|-----------------|-----------------------------|----------------------------------|
| 1 | VAP | Medium | 575000 | 0.171 | 0.073 |
| 2 | VAP | Low | 2500000 | 0.126 | 0.054 |
| 3 | VAP | High | 217000 | 0.203 | 0.087 |
| 4 | VAP | Peak | 139000 | 0.288 | 0.114 |
| 5 | VAP | Low | 2520000 | 0.124 | 0.052 |
| 6 | VAP | Medium | 253000 | 0.173 | 0.071 |
| 7 | VAP | High | 269000 | 0.207 | 0.086 |
| 8 | VAG | Medium | 941000 | 0.136 | 0.061 |
| 9 | VAG | Medium | 1063624 | 0.140 | 0.065 |
| 10 | VAG | High | 126350 | 0.185 | 0.083 |
| 11 | VAG | Low | 3921275 | 0.101 | 0.048 |
| (†)13 | VAG | Low | 5133411 | 0.103 | 0.046 |
| 14 | VAG | High | 247441 | 0.180 | 0.074 |
| 15 | CA | 2.2 | 740735 | 0.085 | 0.085 |
| (†)16 | CA | 1.7 | 5269515 | 0.065 | 0.065 |
| 18 | CA | 1.95 | 1027847 | 0.074 | 0.074 |
| 19 | CA | 2.6 | 291260 | 0.099 | 0.099 |
| 20 | VA2 | - | 1131716 | 0.069 | 0.061 |
| 21 | VA2 | - | 4880396 | 0.069 | 0.061 |
| (†)22 | VA2 | - | 5024628 | 0.068 | 0.061 |
| 23 | VA2 | - | 913856 | 0.069 | 0.061 |
| 24 | VA2 | - | 321904 | 0.069 | 0.061 |
| 25 | CA | 2.8 | 105769 | 0.109 | 0.109 |
| 26 | CA | 2.8 | 144230 | 0.115 | 0.115 |
| 27 | CA | 1.8 | 1367448 | 0.073 | 0.073 |
| 28 | CA | 1.7 | 512749 | 0.065 | 0.065 |
| (†)29 | CA | 1.7 | 5000000 | 0.068 | 0.068 |
| (†)30 | CA | 1.7 | 5000000 | 0.067 | 0.067 |

(*) The severity for the CA experiments corresponds to the prescribed displacement amplitude.

(†) Run-out experiment, where the number of cycles exceeded the run-out limit of 5 million cycles. The fatigue tests were stopped prior to leakage.

2.3 Objectives

The maximum nominal strain in the piping components occurred at the outside, which made outside initiation most likely, as reported in [2]. The assumption that the fatigue cracks all initiated from the outside could however not be verified. The current study is a continuation of the work performed in [2, 3]. The current work aims in particular at

- increasing knowledge on where fatigue cracks initiate and how propagation occurs in welded austenitic stainless steel pipes,
- improving understanding of fatigue critical points in welds,
- improving understanding of the link between weld quality and fatigue resistance.

A fractographic analysis using microscope is to be performed for each of the 28 considered test specimens. The piping components will be pulled apart statically in order to allow detailed characterization and investigation of the fatigue crack fracture surfaces.

3 Fractographic Study

It is of importance to reveal fatigue fracture surfaces without damaging them during the separation process, therefore the test specimens were pulled apart statically using a servo-hydraulic testing machine, which prevented contact between opposing fracture surfaces. The test specimens then experienced ductile fracture and large local deformations. These newly created ductile fracture surfaces are however inclined and can therefore clearly be distinguished from the planar fatigue crack surfaces.

The fracture surfaces were then cut away from the remaining piping component and subjected to visual fractographic examination using an optical microscope. The selected investigation method had a minimum detectable flaw size of about 0.1 mm. The fatigue initiation position of the fatigue crack causing leakage was estimated, as well as the fatigue crack lengths on the inside and outside of the specimens. Only angular measurements were performed as these were unaffected by local deformations of the piping component introduced during the separation process. A cylindrical coordinate system (r, φ, z) was introduced with reference point the center of the pipe's cross-section and $\varphi = 0$ indicating the circumferential position of the strain gage, see Figure 2. The strain gage was situated in the bending plane of the specimen on the side closest to the servo-hydraulic testing machine. The z-axis coincides with the axis of the specimen.

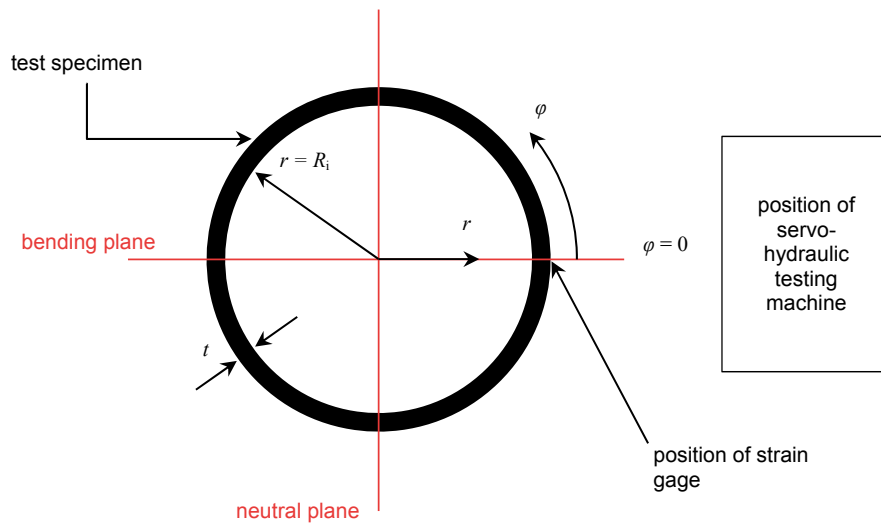


Figure 2 Polar coordinate system introduced in the cross-section of the test specimen.

4 Results

The fracture surfaces of a total of 28 test specimens were examined:

For the 5 run-out specimens the fractographic investigation revealed no fatigue cracks. All fracture surfaces were characterized by ductile failure. During the separation process the run-out specimens failed either in the heat affected zone (HAZ) or in the base material of the piping component close to the weld.

For the remaining 23 piping components that actually failed as leakage was detected, different features were determined characterizing both fatigue initiation and propagation, see Table 3. The fatigue initiation position was estimated with its radial, circumferential and axial position using the polar coordinate system defined in Figure 2, and the fatigue crack lengths on the inside (l_{in}) and outside (l_{out}) of the piping component at the end of the fatigue test were calculated. During the design of the experimental set-up special care was taken to minimize and to some extent prevent difficulties such as wear at connections, mechanical play and complex stress distributions. The experimental set-up allowed for flexible and convenient testing. The design of the piping components and test equipment ensured that the fatigue process was governed by the local weld conditions, which is also the case for real components.

4.1 Fatigue Initiation

The fatigue cracks initiated either from the inside or the outside of the piping component, see Figure 3. Internal fatigue initiation, at $R_i < r < R_i + t$, from for instance an interior material defect included in the pipe wall was not observed during the current investigation. Initiation from the inside corresponds to initiation from the weld root at $r = R_i$. As the test specimens were pressurized with water, such fatigue cracks were then in contact with water during the entire damage process, as opposed to fatigue cracks that initiated from the outside or weld cap, at $r = R_i + t$. This difference in environment most likely explains the observed difference in coloring of the fatigue crack fracture surfaces. The fatigue fracture surfaces of cracks initiated from the inside were in general slightly darker, when compared to those initiating from the outside.



(a) Specimen 8.



(b) Specimen 14.

Figure 3 Fatigue crack initiation from (a) inside, and (b) outside of the piping component. The (red) arrow indicates the propagation direction.

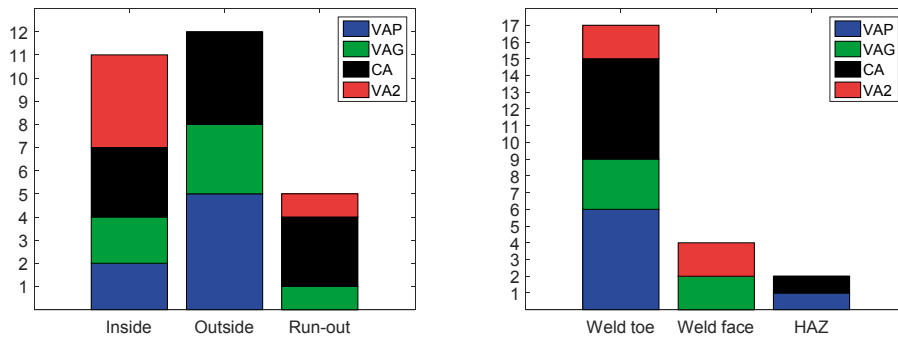
Table 3 Fractographic results for the performed fatigue tests.

| Pipe ID | Load type | Severity | Fatigue initiation | | | Fatigue Propagation | |
|---------|-----------|----------|--------------------|------------------|-------------------------------|---------------------|-----------|
| | | | Radial position | φ_{init} | Axial position ^(¶) | l_{in} | l_{out} |
| | | | | [°] | | [mm] | [mm] |
| (§)1 | VAP | Medium | outside | 34 | weld toe | 133 | 147 |
| 2 | VAP | Low | inside | 0 | weld toe | 8 | 2 |
| 3 | VAP | High | outside | 161 | weld toe | 2 | 17 |
| 4 | VAP | Peak | outside | 30 | weld toe | 7 | 11 |
| 5 | VAP | Low | inside | 17 | HAZ | 21 | 7 |
| 6 | VAP | Medium | outside | 17 | weld toe | 5 | 25 |
| 7 | VAP | High | outside | 8 | weld toe | 3 | 13 |
| 8 | VAG | Medium | inside | -15 | weld face | 8 | 3 |
| (§)9 | VAG | Medium | outside | 0 | weld toe | 75 | 82 |
| 10 | VAG | High | outside | 12 | weld toe | 6 | 26 |
| 11 | VAG | Low | inside | 26 | weld face | 10 | 11 |
| 13 | VAG | Low | - | - | - | - | - |
| 14 | VAG | High | outside | -21 | weld toe | 6 | 15 |
| 15 | CA | 2.2 | inside | 172 | weld toe | 17 | 6 |
| 16 | CA | 1.7 | - | - | - | - | - |
| 18 | CA | 1.95 | inside | -148 | weld toe | 8 | 4 |
| 19 | CA | 2.6 | outside | 6 | weld toe | 4 | 21 |
| 20 | VA2 | - | inside | 8 | weld toe | 14 | 10 |
| (‡)21 | VA2 | - | inside | -31 | weld face | 8 | 4 |
| 22 | VA2 | - | - | - | - | - | - |
| (‡)23 | VA2 | - | inside | 8 | weld face | 8 | 4 |
| 24 | VA2 | - | inside | 171 | weld toe | 13 | 4 |
| 25 | CA | 2.8 | outside | 8 | weld toe | 8 | 15 |
| (§)26 | CA | 2.8 | outside | 0 | weld toe | 45 | 58 |
| 27 | CA | 1.8 | outside | -149 | weld toe | 2 | 9 |
| 28 | CA | 1.7 | inside | 9 | HAZ | 12 | 6 |
| 29 | CA | 1.7 | - | - | - | - | - |
| 30 | CA | 1.7 | - | - | - | - | - |

(‡) The identifying markings of these two specimens were unfortunately lost after removing the fracture surfaces from the test specimens. They were then re-allocated a new pipe ID, hence a mix-up cannot be ruled out.

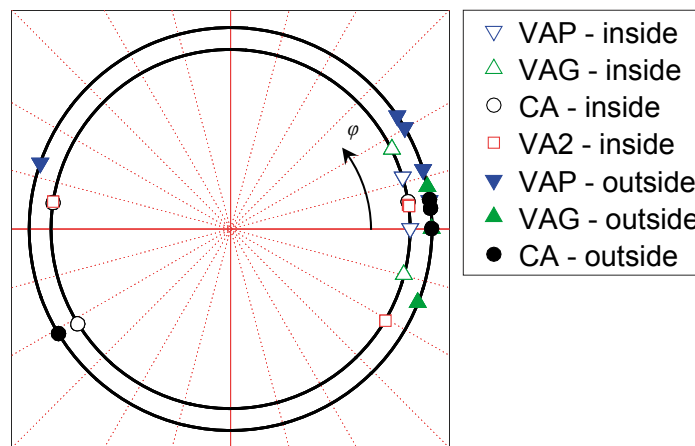
(§) These three specimens were subjected to continued fatigue crack growth after leakage was detected, resulting in large fatigue cracks covering the cross-section of the specimens.

(¶) Weld toe designates here both weld cap toe and weld root toe; Weld face designates here both weld cap face and weld root face.



(a) Radial position of fatigue initiation and run-outs.

(b) Axial position of fatigue initiation.



(c) Fatigue initiation position for different load types superimposed to specimen cross-section.

Figure 4 Position of damage initiation for the different test specimens that failed due to fatigue.

From the 23 test specimens that failed due to fatigue about one half initiated from the inside, whereas the other half presented initiation from the outside, see Figure 4 (a). It occurred also that a specimen presented multiple initiation sites with multiple propagating fatigue cracks. Despite the presence of numerous cracks, only one single dominant crack was responsible for causing leakage by penetrating the entire wall thickness of the piping component.

The circumferential position of fatigue initiation φ_{init} was estimated for the fatigue crack that caused leakage, see Table 3. The fatigue initiation positions for the failed specimens are illustrated graphically in Figure 4 (c). It can be observed that the initiation tended to occur in the vicinity of the bending plane, where the strain amplitudes reached maximal values. A dissymmetry can though be noted, as the majority of the fatigue initiations occurred near $\varphi = 0$, and only few fatigue cracks started near $\varphi = \pm 180^\circ$. This observation is most likely related to a relative difference in load amplitude of about 8% between these positions for the considered piping component and experimental set-up. Indeed at $\varphi = 0$ the membrane load introduced by the applied force on the fixtures is in phase with the bending load, resulting in an increased load amplitude, whereas at $\varphi = \pm 180^\circ$ this particular membrane load and the bending load have opposite phase resulting in a lower load amplitude.

The fatigue initiation position occasionally also observed to coincide with the weld start/stop position, see for instance specimen 14 in Figure 5 (a). The circumferential fatigue initiation position was affected by the detrimental residual stress state at the weld start/stop position. Finite element simulations have shown increased residual stresses at the start/stop position of the weld [4], which can explain localization of fatigue initiation.

Finally the axial position of the estimated initiation sites was determined. Initiation of fatigue cracks in the considered welded piping component was observed to potentially occur at three different distinct positions:

- at a weld toe, including both weld root toe (on inside) and weld cap toe (on outside),
- at a weld face, including the weld root face (on inside) and the weld cap face (on outside),
- in the heat affected zone (HAZ).

These designations are illustrated in Figure 6 and used in both Table 3 and Figure 4 (b). The latter clearly illustrating the weld toe as the more critical position regarding fatigue initiation. All the fatigue cracks that started from the outside were indeed initiated at a weld cap toe, see illustrated in Figure 5 (a). No fatigue cracks started from the weld cap face or HAZ on the outside of the piping component. Cracks starting from the inside of the welded pipe initiated generally from a weld root toe or the weld root face. The latter is illustrated in Figure 5 (b). Still some cracks also initiated from the HAZ on the inside of the specimen.



(a) Specimen 14.



(b) Specimen 8.

Figure 5 Illustration of (a) weld cap toe crack initiation and (b) weld root face crack initiation, with views on the inside and outside of the weld joint.

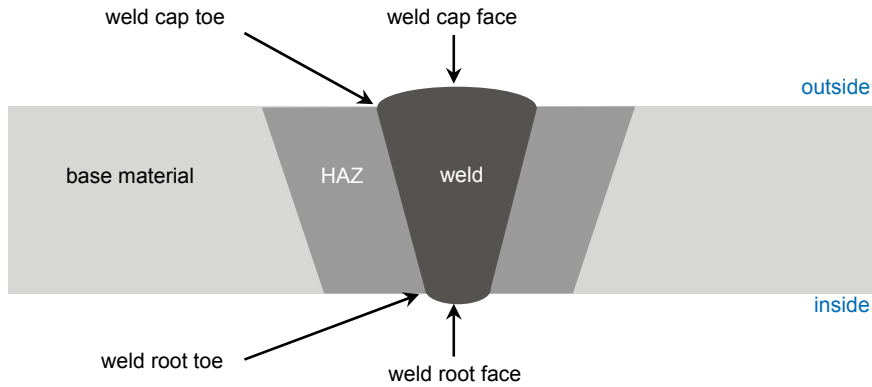
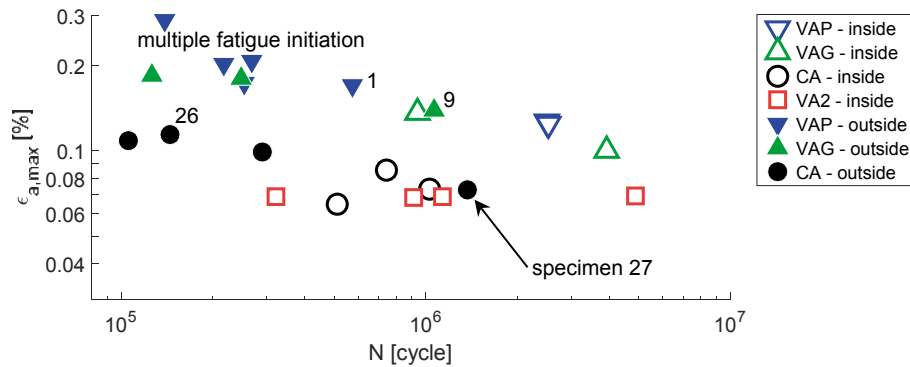
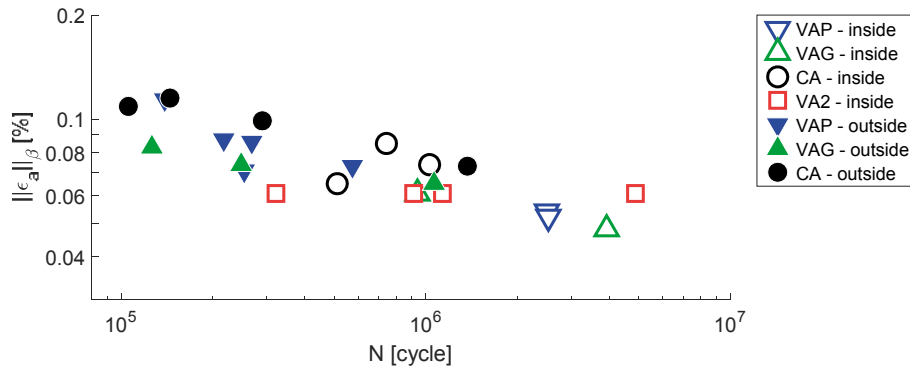


Figure 6 Weld nomenclature used in current study.



(a) Maximal nominal strain amplitude vs total number of cycles.



(b) Beta-norm vs total number of cycles.

Figure 7 Radial fatigue initiation position in relation to load and number of cycles for the failed tests.

Figure 7 represents a nominal measure of the load amplitude as function of the total number of cycles the specimen was subjected to prior to leakage detection. Figure 7 (a) shows the maximal nominal strain amplitude and the beta-norm defined in [2] is represented in Figure 7 (b). The strain measures in Figure 7 (a) and (b) are both based on the recorded nominal strain for each piping component using a strain gage situated in the bending plane, see Figure 2. These strains do obviously differ from the local strains the material near the welding joint experienced due to the presence of the weld material and stress concentrations at the junctions of the joint. Figure 4 (a) did not directly reveal a clear relation between radial fatigue initiation position and load type, however Figure 7 points at the radial fatigue initiation position being related to the severity of the load type. It can namely be observed that initiation

from the outside of the welded piping component occurred mainly for high strain amplitudes, resulting in low fatigue life. All test specimens with a total fatigue life $N < 3 \times 10^5$ show fatigue cracks initiating from the outside. Fatigue crack initiated from the inside of the test specimen occurred however with smaller strain amplitudes inducing higher fatigue life. Thus the damage process acting in the low cycle fatigue (LCF) regime differs distinctively from the one prevailing at HCF.

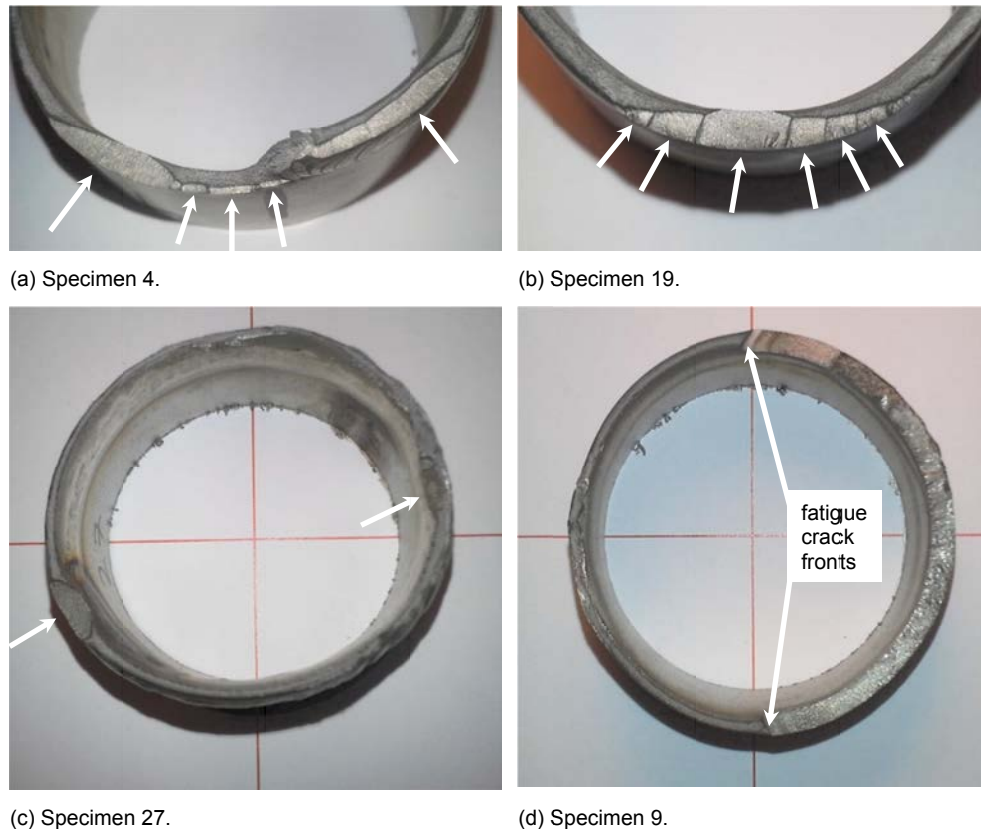


Figure 8 Illustration of multiple fatigue initiation sites, adjacent fatigue cracks and continued fatigue crack growth.

Table 3 represents the data for the dominant fatigue crack inducing leakage, but for several specimens multiple fatigue initiation sites were observed, see in particular Figure 8 (a) and (b), which resulted in separate or adjacent fatigue cracks. This occurred mainly in combination with initiation from the outside, which was identified as the prevailing initiation position at LCF. In particular multiple fatigue initiation always occurred for specimens subjected to large peak loads, i.e. with maximum nominal strain amplitudes larger than 0.18%, see Figure 7(a). As an example specimen 4 in Figure 8 (a) may be mentioned. This specimen experienced the largest nominal strain amplitude during the test program, which explains the large number of distinct fatigue cracks that initiated. The beta-norm in Figure 7(b) being an equivalent strain measure cannot reveal this feature related to fatigue initiation and was found more appropriate for the study of propagation.

Specimen 27 may appear as a clear exception in Figure 7(a), as this piping component presented a dominant fatigue crack causing leakage starting from the outside although being subjected to a HCF load, but the investigation of its fracture surface also revealed at a different circumferential position a well-developed fatigue crack that had initiated from the inside, see Figure 8 (c), which agrees well with the prevailing damage process at HCF. The fatigue crack that started from the inside did not penetrate the entire wall thickness of specimen 27, but reached an

estimated crack depth of at least $0.8t$. The atypical initiation from the outside may be related to an event during welding, as suggested by the enhanced oxidation markings illustrated in Figure 9. A minor weld repair or improvement may have been performed at this location, which may be related to the somewhat increased weld cap height at this particular location. The modified residual stress state and expected higher stress concentration on the outside may be responsible for inducing fatigue initiation at this particular location.

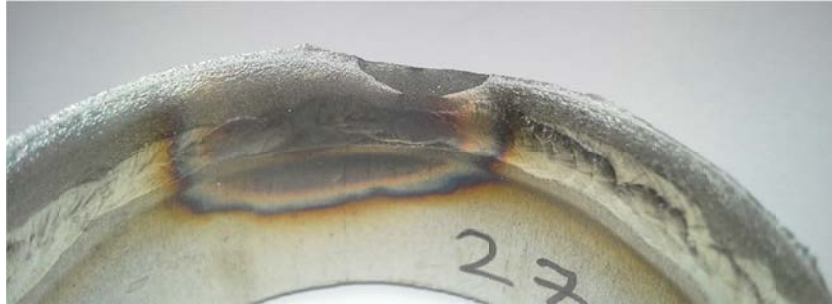


Figure 9 Weld oxidation region coinciding with the fatigue initiation position from the outside for specimen 27.

Specimens 1, 9 and 26 have been subjected to continued fatigue crack growth even after leakage was detected and when the internal pressure of 70 bar no longer could be sustained. The data points for these three specimens are marked in Figure 7 (a). When fatigue crack propagation was allowed to be continued the fatigue crack progressed to cover a major part of the specimens' cross-section, see for instance Figure 8(d), where the fatigue crack in specimen 9 almost covers half of its cross-section. The fracture surfaces for these three specimens did therefore no longer represent the state at leakage. Given the negative load ratio, continued fatigue testing introduced considerable wear of the fracture surfaces. The sustained damage of the fracture surfaces rendered some features, such as the initiation position, uncertain or at least more challenging to determine. This may explain why both specimens 1 and 9 seem to present atypical radial initiation positions in Figure 7 (a).

4.2 Fatigue Propagation

Once a fatigue crack is initiated in the wall of the pipe, a semi-elliptical crack is formed and further propagation through the wall thickness occurs until leakage.

4.2.1 Fatigue Crack Shape at Leakage

The examination of the fracture surfaces allowed estimation of the crack length both on the inside, l_{in} , and outside, l_{out} , of the tested piping components, see Table 3. One can note that the crack length on the initiation side always exceeded the crack length created on the penetration side. This is visually illustrated by the typical crack shapes presented in Figure 3, but can also be observed in Table 4, where median crack lengths are reported. Note that data for specimens 1, 9 and 26 was not included, as they had been subjected to continued fatigue testing. Table 4 also illustrates an essential difference in crack shape depending on the radial initiation position. Fatigue cracks starting from the outside have larger crack length on the initiation side at leakage than those that started from the inside.

Table 4 Median crack lengths in mm at leakage.

| Radial initiation position | Initiation side | Penetration side |
|----------------------------|-----------------|------------------|
| Inside | 10 | 4 |
| Outside | 15 | 5 |
| Inside + Outside | 13 | 4.5 |

During propagation under reversed bending load these two types of fatigue cracks experience a different nominal strain field variation. A crack starting from the inside will therefore be more prone to propagate in depth towards the more highly strained regions near the outside of the pipe wall. Cracks initiating from the outside will however be more prone to grow along the outer surface, where the strain amplitudes are larger than deeper inside the pipe wall. Increased circumferential crack growth induces more flattened semi-elliptical crack shapes, i.e. with high eccentricity, as observed for fatigue cracks starting from outside. Visual inspection of the crack shapes at leakage, see Figure 3, confirms the results presented in Table 4. Cracks starting from the inside tended to have a semi-elliptical crack shape with low eccentricity, i.e. close to semi-circular crack shape, see Figure 3 (a), whereas the semi-elliptical crack shape for cracks starting from the outside had larger eccentricity, see Figure 3 (b), giving larger crack lengths on the outside. These observations can be explained by the prevailing stress/strain state, but also by the presence of adjacent cracks due to multiple initiations, which was common for initiation from the outside.

On the penetration side the median crack length was however similar at leakage, see Table 4. Fatigue failure was defined to have occurred when the internal pressure of 70 bar could no longer be sustained. This practical and realistic failure criterion seems to be equivalent to a crack length on the penetration side of approximately 4.5 mm, see Table 4.

4.2.2 Fatigue Crack Interaction

Multiple initiation and consecutive propagation of multiple fatigue cracks has been observed in the investigated specimens. It was observed that fatigue cracks that started at nearby positions could either merge or inhibit each other's growth. The former case occurred when the initiation sites were situated at similar axial positions, hence the planar fatigue cracks propagated in almost the same plane. This facilitated merging of the fatigue cracks and resulting in a larger penetrating crack. The latter case was observed when fatigue cracks initiated at close by circumferential position but at different axial positions. As a result the fatigue cracks grew on different planes and did not merge. Indeed, ligaments with ductile fracture, created when the specimens were pulled apart, separated the different fatigue cracks. The growth of adjacent fatigue cracks limited the circumferential growth of the penetrating crack.

5 Discussion

The studied test specimens are thin-walled welded piping components. The small wall thickness of the specimens gave a relative difference in nominal axial strain amplitude of about 11% between the inside and the outside. The weld joint toes, present both on the inside and outside represent strain concentrations, which may however be quite different depending on the quality of the performed weld. Depending on the magnitude of these strain concentrations, either the inside or outside of the specimens may therefore experience the larger strain amplitude, which may consequently induce initiation of a fatigue crack. Fatigue cracks starting from the inside of the specimen are thus not to be excluded for thin-walled welded piping components, which was illustrated by the fractographic observations in the current study. Increased wall thickness will contribute to increasing the nominal axial strain amplitude difference between the inside and outside. As a result for thick-walled welded piping components, fatigue initiation from the outside can be expected to occur predominantly.

It was previously in [2] assumed that all the fatigue cracks had initiated from the outside, where the maximum nominal strain was maximal, and hence avoiding environmental effects as water contact only occurred in the final stage of the damage process, when the pipe wall was penetrated. With the current study, this assumption was found valid only for the test specimens that had been subjected to less than 3×10^5 total number of cycles, i.e. a LCF load. Meanwhile, it was observed that for HCF loads, the fatigue cracks generally started from the inside, thus with (pressurized) water contact during the entire damage process. The presence of water in the crack may have influenced the damage process somewhat, given for instance the different observed coloring of the fracture surfaces, but the potential environmental effects on the fatigue life test results can still be assumed negligible. Indeed, several necessary conditions for environmental fatigue were not fulfilled [5]. In particular the fatigue tests were performed at room temperature, which is far below the threshold temperature introduced in [5], below which environmental effects are considered to be insignificant.

Although both radial initiation positions, i.e. inside and outside, may practically experience comparable strain amplitudes for the considered test specimens, the residual stresses at these locations will differ. Residual stresses are introduced by the welding process and for thin-walled pipes a circumferential butt weld induces an approximately linear axial residual stress through the thickness of the weld joint. Near the capping the residual stresses are expected to be compressive, whereas tensile residual stresses are introduced at the weld root [6, 7]. The latter case is clearly more detrimental to fatigue initiation and propagation, as the mean stress near the weld root will be larger than the one at the weld cap. Increased tensile residual stresses are introduced at the weld start/stop position [4], which will also alter the mean stress. As a result the mean stress is expected to differ considerably between the inside and outside of the test specimen, which will consequently contribute to localize fatigue initiation and affect the fatigue crack growth rates at the respective positions. Once a fatigue crack has been initiated on the inside of the specimen the internal pressure will further increase the mean load by means of a constant crack face pressure.

As illustrated in Figure 7 (a), different fatigue damage processes were identified to act at LCF and HCF. Caution is therefore recommended when extrapolating results for instance obtained for LCF to the HCF domain or vice versa. Similarly the effect of solutions to improve fatigue life of the piping component will differ considerably depending on the prevailing damage process. Removal of the weld cap by grinding or any other finishing operation is often proposed to be beneficial to the fatigue resistance of a piping component. This is indeed the case as long as

fatigue initiation from the outside is the prevailing mechanism. However, at HCF it is expected to have no effect and may even be detrimental to the fatigue strength of the studied piping component. Weld cap removal removes the weld cap toes which represented geometric strain concentrations on the outside of the joint. It is thus in this way clearly detrimental to fatigue crack initiation from the outside, but does not affect the weld toes at the root. The cap removal induces also a redistribution of the weld residual stresses, which may lead to increased tensile mean stress at the root, contributing this way to possible root fatigue initiation. The extent of the success of an external treatment of the weld joint will thus be limited by the fatigue life related to fatigue cracks starting from the inside.

6 Conclusions

A fractographic examination using microscope was performed for each of the 28 considered thin-walled welded piping components that had been subjected to different fatigue load types, both constant and variable amplitude. The obtained findings and results of the performed study are as follows:

- The weld toes near the bending plane on both the inside and outside of the weld joint were the most critical regions for fatigue initiation.
- Increased weld residual stresses at the weld start/stop position can contribute to initiation and growth of a fatigue crack.
- The radial fatigue initiation position, i.e. on the inside or outside of the piping component, was not directly related to the load type, but to its severity.
- The maximum strain amplitude was found more suitable to explain fatigue initiation features, such as multiple initiation sites.
- Initiation of multiple, adjacent fatigue cracks, was observed for specimens subjected to large strain amplitudes (high or peak loads).
- Wall penetration tended to be caused by a single dominant fatigue crack, with or without merging with quasi-coplanar adjacent cracks.
- Two distinct fatigue failure mechanisms with separate initiation sites were identified for the considered thin-walled welded piping component.
- Fatigue initiation from the outside of the weld joint occurred predominantly at LCF, giving fairly flattened semi-elliptical fatigue crack shapes.
- Fatigue initiation from the inside of the weld joint or weld root was the dominant fatigue failure mechanism at HCF, inducing often close to semi-circular fatigue crack shapes.
- The weld cap removal is expected to improve fatigue life for LCF applications, but not for HCF applications with weld root initiation.
- The effectiveness of outer surface finishing operations of the weld joint to increase fatigue resistance, will for LCF applications eventually be limited by fatigue initiation from the weld root. For HCF applications weld cap removal may even affect fatigue resistance negatively due to residual stress redistribution.
- Even with water contact during major parts of the damage process, environmental effects on the recorded experimental fatigue life are still assumed to be insignificant given the considered test conditions.

7 Recommendations

The performed investigation can be continued or complemented with one or more of the following actions:

- The combination of small wall thickness and the presence of a weld joint in as-welded condition, allowed competition between fatigue initiation from the inside and outside. The distinct observation of different initiation sites for LCF and HCF could not be explained. The transition between the fatigue failure mechanisms is presumed specific to the investigated piping component, and may be related to non-linear material behavior and/or the residual stress field. Fatigue tests of welded piping components with different wall thickness may quantify the expected shift of the transition between the identified fatigue mechanisms. Such an experimental study will contribute to finding an explanation and allow generalization of the current observations to other welded piping components.
- The current investigation considered a welding joint in as-welded condition. Fatigue experiments on welded piping components with removed weld cap may contribute to quantify the effect of an outer surface finishing operation on the fatigue resistance of a piping component.
- Fatigue experiments on welded piping components with weld start/stop positions at different circumferential positions allow to determine the extent of the expected detrimental effect on fatigue life of the weld residual stress at the weld start/stop position.

8 Acknowledgement

The Swedish Radiation Safety Authority is gratefully acknowledged for the financial support.

9 References

- [1] ASME, "Boiler and Pressure Vessel Code, Section III, Rules for Construction of Nuclear Facility Components," 2013.
- [2] M. Dahlberg, D. Hannes and T. Svensson, "Evaluation of fatigue in austenitic stainless steel pipe components," *SSM* 2015:38, 2015.
- [3] T. Svensson, D. Hannes, P. Johannesson, M. Dahlberg and A. Anderson, "Three HCF models for strain fatigue life of welded pipes in austenitic stainless steel," *Procedia Engineering*, vol. 101, pp. 476-484, 2015.
- [4] E. Bonnaud and J. Gunnars, "Three Dimensional Weld Residual Stresses Simulations of Start/Stop and Weld Repair Effects," *Procedia Engineering*, vol. 130, pp. 531-543, 2015.
- [5] O. Chopra and W. Shack, "Effect of LWR Coolant Environments on the Fatigue Life of Reactor Materials," NUREG/CR-6909, 2007.
- [6] P. Dillström, M. Bergman, B. Brickstad, W. Zang, I. Sattari-Far, P. Andersson, G. Sund, L. Dahlberg and F. Nilsson, "A combined deterministic and probabilistic procedure for safety assessment of components with cracks - Handbook," *SSM* 2008:01, 2008.
- [7] W. Zang, J. Gunnars, P. Dong and J. K. Hong, "Improvement and validation of weld residual stress modelling procedure," *SSM* 2009:15, 2009.



2016:28

The Swedish Radiation Safety Authority has a comprehensive responsibility to ensure that society is safe from the effects of radiation. The Authority works to achieve radiation safety in a number of areas: nuclear power, medical care as well as commercial products and services. The Authority also works to achieve protection from natural radiation and to increase the level of radiation safety internationally.

The Swedish Radiation Safety Authority works proactively and preventively to protect people and the environment from the harmful effects of radiation, now and in the future. The Authority issues regulations and supervises compliance, while also supporting research, providing training and information, and issuing advice. Often, activities involving radiation require licences issued by the Authority. The Swedish Radiation Safety Authority maintains emergency preparedness around the clock with the aim of limiting the aftermath of radiation accidents and the unintentional spreading of radioactive substances. The Authority participates in international co-operation in order to promote radiation safety and finances projects aiming to raise the level of radiation safety in certain Eastern European countries.

The Authority reports to the Ministry of the Environment and has around 300 employees with competencies in the fields of engineering, natural and behavioural sciences, law, economics and communications. We have received quality, environmental and working environment certification.

Strålsäkerhetsmyndigheten
Swedish Radiation Safety Authority

SE-171 16 Stockholm
Solna strandväg 96

Tel: +46 8 799 40 00
Fax: +46 8 799 40 10

E-mail: registrator@ssm.se
Web: stralsakerhetsmyndigheten.se